

Science Forum (Journal of Pure and Applied Sciences)

journal homepage: https://atbu.edu.ng/science-forum/



Migmatite morphologies and their potential impact on groundwater availability using hydrostructural approach: A case study of Rimin Zayam migmatitic terrane



Faisal Abdullahi^{1*}, Ahmed Isah Haruna¹, Tahir Garba¹, Maimunatu Halilu², Amina Ali³, Isah Yahuza⁴

- ¹ Department of Applied Geology, Abubakar Tafawa Balewa University, Bauchi, Nigeria
- ² Department of Geology, Moddibo Adama University, Yola, Nigeria
- ³ National Centre for Petroleum Research and Development ATBU Energy Commission of Nigeria, Nigeria
- ⁴ Department of Civil and Environmental Engineering, Airforce Institution of Technology Kaduna, Kaduna, Nigeria

ABSTRACT

The groundwater occurrence, movement, and potential in basement rock terrain are controlled by geological structures like foliations, faults, shear, and folds which are commonly referred to as lineaments revealing that migmatite terrane serves as a conduit for migration has exhibited variable yields of groundwater movement. Major targets in groundwater exploration surveys in basement terrains occur in areas having foliation, weathering of considerable thickness, and/or where fracturing and jointing. The investigation discovered two significant fracture types for the area, low yield, and high yield, which run in the NW-SE directions, foliation plane (NNE-SSW and E-W) (conduit) as well as a structurally controlled drainage pattern. Because their presence is structurally driven, groundwater exploration in the area should be centered along NW-SE and NNE-SSW directions (predominantly), high-yield fracture is attenuated to metatexite migmatite and low yield mostly associated with diatexite trending NW-SE and NE-SW cross-cutting the foliation in the migmatite. The results reveal a good agreement between the trends of fractures derived from the surface manifestation and foliation for groundwater availability making high foliation indicate intense fracturing and thus, indicate areas of high groundwater potentiality. It may be concluded that the occurrence, distribution, and movement of groundwater are influenced and impacted by geological structures which have direct control as well as lithology. This research has improved our understanding of groundwater occurrence and distribution.

ARTICLE INFO Artcle history:

Received 14 January 2023 Received in revised form 13 February 2023 Accepted 14 February 2023 Published 06 July 2023 Available online 06 July 2023

KEYWORDS

Foliation Fracture Metatexite Diatexite Conduit Groundwater Migmatite

1. Introduction

Geomorphology and structures of an area play important roles in the recharge rates of aquifers, thus giving an indication of the good groundwater prospect of an area. The wide range and distribution of fracture values in the study area are typical of migmatite terrain,

thus, a reason why groundwater potential varies significantly within the different migmatite morphologies. Migmatites are high-temperature metamorphic rocks formed by anatexis (partial melting) in continental middle and lower crusts. As any rock will start to melt at sufficient pressure and temperature conditions, often aided by the influx of fluids, and the

^{*} Corresponding author Faisal Abdullahi 🖾 Faisal Abdullahi 🖾 Department of Applied Geology, Abubakar Tafawa Balewa University, Bauchi, Nigeria.

forming melts depend on the protolith (source rock) composition, migmatites can be very heterogeneous in chemical and mineralogical composition (Sawyer and Brown, 2008). The deformation changes the geometry of the rocks by folding, transposition, and boudinage, which result in morphological and/or structural complexity that adds to further petrological heterogeneity. Migmatites are subdivided into metatexites and diatexites (Brown, 1973; Sawyer, 1996, 2008a, 2008b) based on first-order morphology. Where the migmatitic boundary is present, the rock is called a metatexite, where the boundary is disrupted due to higher volumes of melt; it is called diatexite. Metatexite represents small to moderate degrees of partial melting, in which a pervasive melt fraction does not develop throughout the rock (Brown, 1973, 2001a, 2001b; Sawyer, 1998). In contrast to metatexites, diatexites have a composition similar to granite plutons, represent high degrees of partial melting, and contain a variable amount of restite; pre-migmatization structures are destroyed and homogenization and coarsening of the textures occurred. Foliation belongs to a group of structures that are called pervasive, i.e., structures that do not occur as individual features (like fracture or bedding planes) but rather affect the whole mineral aggregate or grain (Passchier and Trouw 2005). Such structure is characteristic of Rimin Zayam migmatitic rocks.

Field geologic mapping serves as the first-hand method used to determine the distribution and variability and relative intensity of structures that serve as a conduit for potential groundwater availability at the outcrop scale. Migmatite morphologies will serve as good water-bearing high permeability rock that will lithologically and structurally control water-bearing zones formed parallel to the foliation and compositional layering (Figs. 8 and 9). The presence of foliation planes and mineral alignation and fractures in the study area within the morphologies of metatexite and diatexite warrant the analysis of a few structures in order to establish the hydrogeological conceptual model of the availability and possible yield capability of the groundwater system in the study area. The outcome of this work will serve as a framework that would guide groundwater potential in basement rock and provide baseline information for relevant agencies in need of structural that for groundwater development both in rural and urban communities and other associated environmental projects.

1.1. Study area

The study area is located within the Pan African Older Granite and lies between latitudes 10°9'00"N and

10°12'30"N and longitudes 9°17'00"E and 9°21'30"E, it is part of the Toro sheet and covers an area of about 53.27 km². The study area is located in Rimin Zavam East of Toro LGA in Bauchi state and is accessible through Bauchi-Jos Road (Fig. 1). The currently accepted location of the studies is based mainly on its lithological, metamorphic, and structural constraints, and its complication by an anastomosing network of high-strain zones (Fig. 3) (e.g., deformation zones) that bound and intersect the various rocks and by a series of deformational and metamorphic overprinting events (Ferre and Caby, 2006) characterized by highland and flat topography with outcrops of low, moderate, and high-level elevation that ranges from 640 m to about 1,020 m (Fig. 4a). River Rimin Zayam is the only major river in the study area and has its snore sources in the highland around the Jos Plateau. It is however fed by many tributaries, and in turn, runs into River Delimi (Fig. 4b). The area is characterized by sheet erosion. The drainage pattern is dendritic (Fig. 4b).

with small streams controlled by foliation planes of the outcrops (structurally controlled).

1.2. Geologic background

The Bauchi situated to the east of the main terrane boundary, includes mostly gneisses and anatexites of metasedimentary origin. The depositional age of the sediments is poorly constrained. No basement–cover relationships have been identified. Work done by Dada and Respaut (1989), Dada et al. (1989), and Ferre et al. (1998, 2002) (Fig. 2).

The Rimi Zayam (Fig. 2) locality exposes garnetbiotite diatexites with a larger number of boudins and xenoliths of metasedimentary rocks among which are quartzites, calc-silicates, and sillimanite-garnet metapelites. These metasedimentary gneisses represent selected layers that have been torn from the surrounding gneisses and they display a strong tectonic fabric different from the foliation of enclosing diatexite, as evidenced by the rotated foliation of the nearly spherical boudins (Ferre and Caby, 2006). The presence of aluminous granitoid was observed and the transition between diatexite was ascertained, and they are garnet-bearing but show replacement by biotite associated with late muscovite. The co-existence of orthopyroxene+mesoperthite—typical of the granulite facies, suggests peak temperatures well above 800°C (Rushmer, 1991). Although the microcline porphyroblasts tend to grow with their longer axes in the plane of the foliation of the rock, the general effect of their development is to obliterate the gneissose

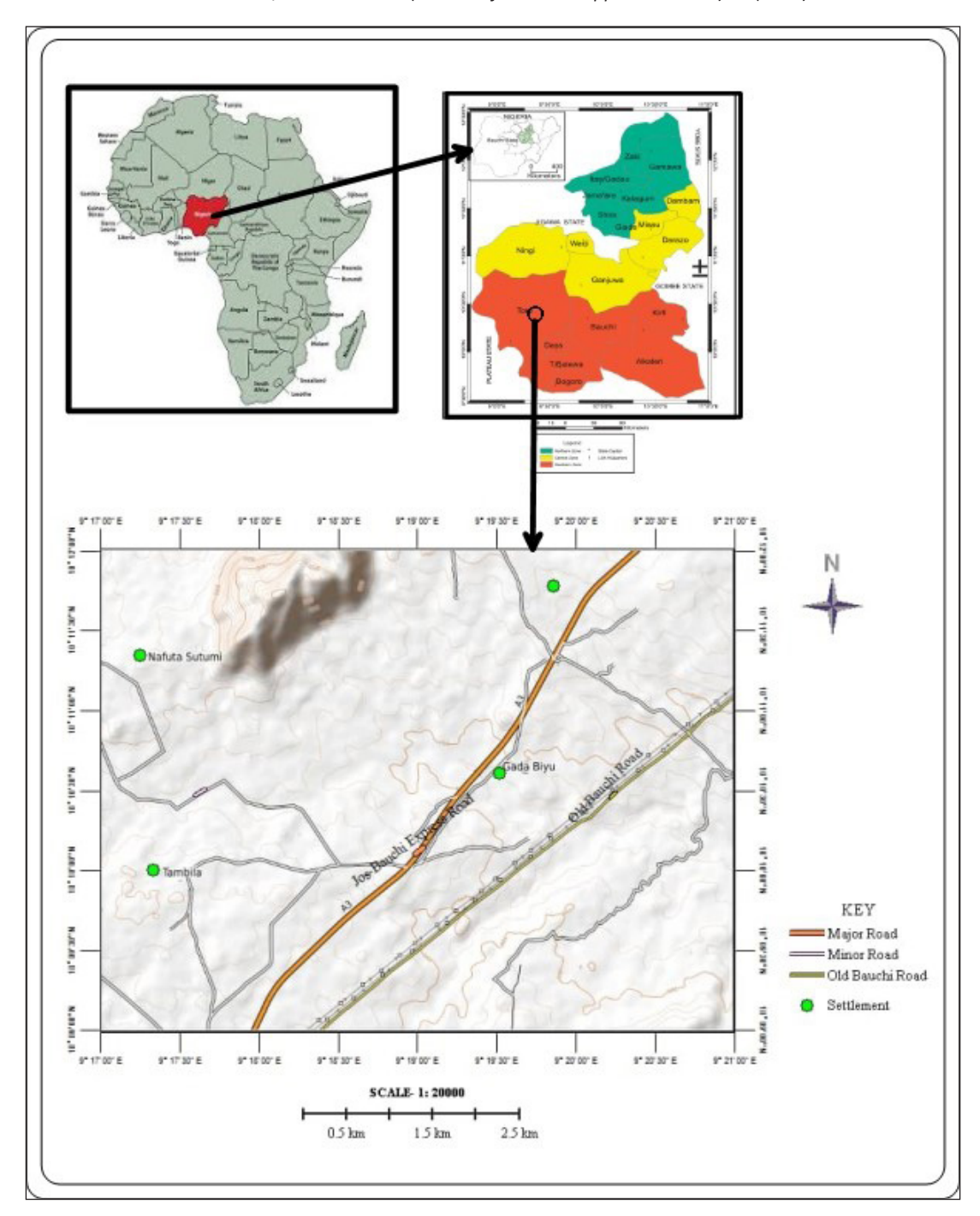


Figure 1. Location map of the study area. Embellished from Arcmap 10.1.

appearance and alter the rock progressively toward one of the granitic aspects (Oyawoye, 1959).

The structural elements in the study area include joints, faults, foliations, and minor folds. Most of these structural elements do not appear on the map due to the scale of the map. Some fault lines that appear on the map are deep-seated in origin and ancient in age and are a result of thermotectonic deformational events mostly of the Pan-African Orogeny (Annor and Freeth,

1985; Rahaman, 1976). The dominant structural trend in the basement is essentially NE–SW and follows the tectonic grain of the schist belt (Dada, 2006; Obiora, 2005). Subordinate directions, which are locally dominant, include E-W and NW-SE. Widespread fracturing occurs throughout the area and follows the orientation of the major faults.

The relic of metasedimentary country rock does not display microstructure but shows strong tectonic

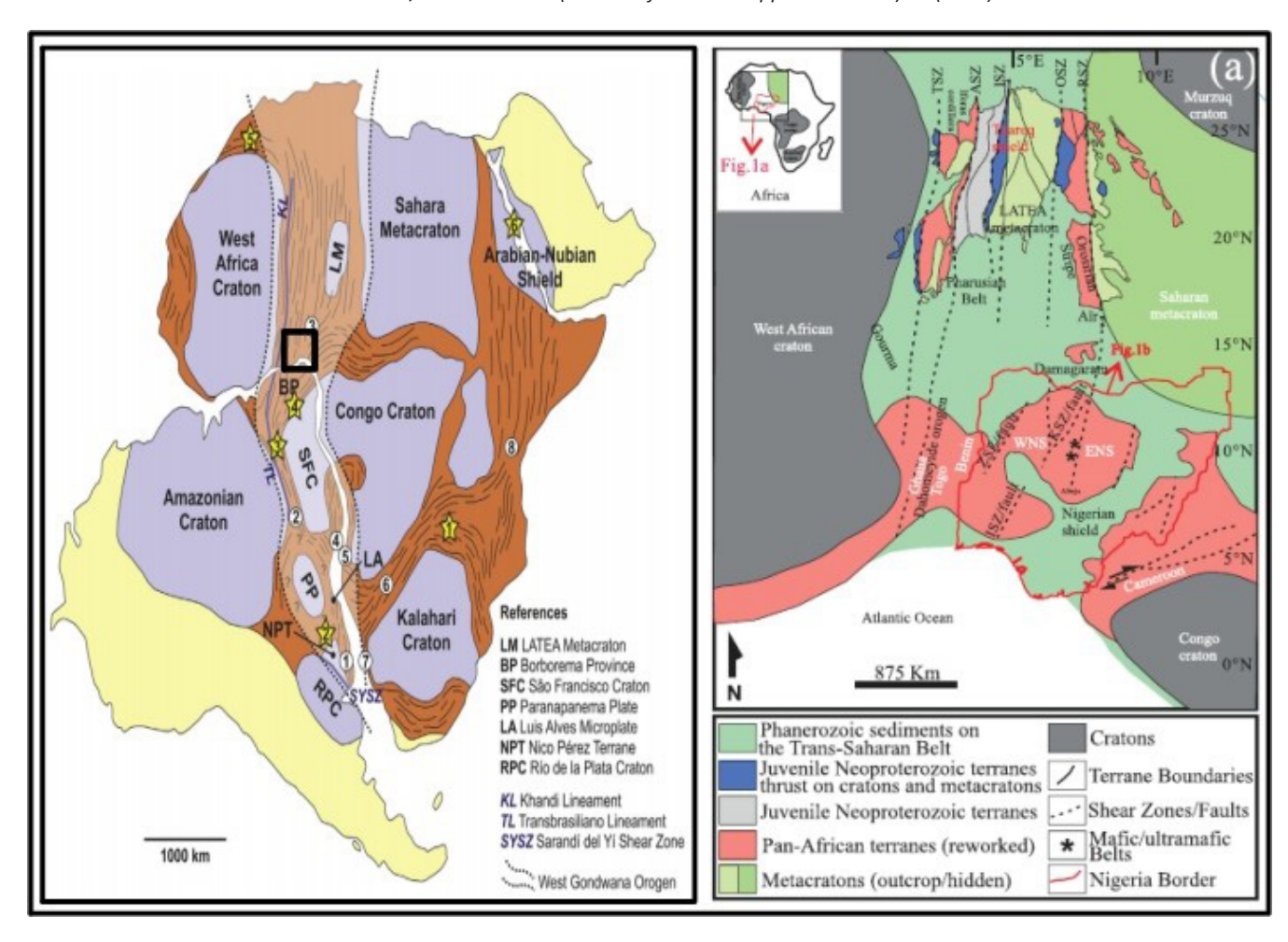


Figure 2. Geology of Nigeria in the context of West Africa (Wright, 1985).

fabrics and similar syn-kinematic mineral assemblages as the country rock. The deformation changes the geometry of the rocks by folding, transposition, and boudinage, which result in morphological and/or structural complexity that adds to further petrological heterogeneity (Ferre and Caby, 2006). The rocks display N-S to NE-SW low-angle foliations affected by open fold. This foliation becomes upright approaching the pluton and locally parallel to their igneous foliation.

2. Materials and Methods

2.1. Data acquisition

Data acquisition is done in surface outcrop, which aims at mapping pervasive structures that provide structural orientation data for areas with impact for a hydrogeological model of migmatite morphology of the study area in connection to providing possible groundwater availability. Parameters such as width, length, and spacing which are important in fracture system

analysis are put into consideration. Trend and attitude readings of foliation and fracture were collected using a compass clinometer and phone base structural software. A rose diagram showing the predominant joint directions was subsequently produced. Software used includes Stereowin, Field Move, Geopaparazzi, Arcgis, Global Mapper, 3D Move, and Surfer v21.

Field geologic mapping was conducted on a scale of 1:12,500 in the northwestern quadrant of the sheet. In order to assess the hydrogeological structural conditions of the different migmatite morphologies, structural measurements of joint and fracture sets were taken where possible.

2.2. 3D terrane analysis

Remote sensing studies involve a production lineament map of the study area. This analysis was carried out by first downloading the digital elevation model (DEM) (Fig. 4) and drainage map (Fig. 5) were products of the study area using Google Earth Engine, TCX converter, and surfer V21 (Kriging and Modeling).

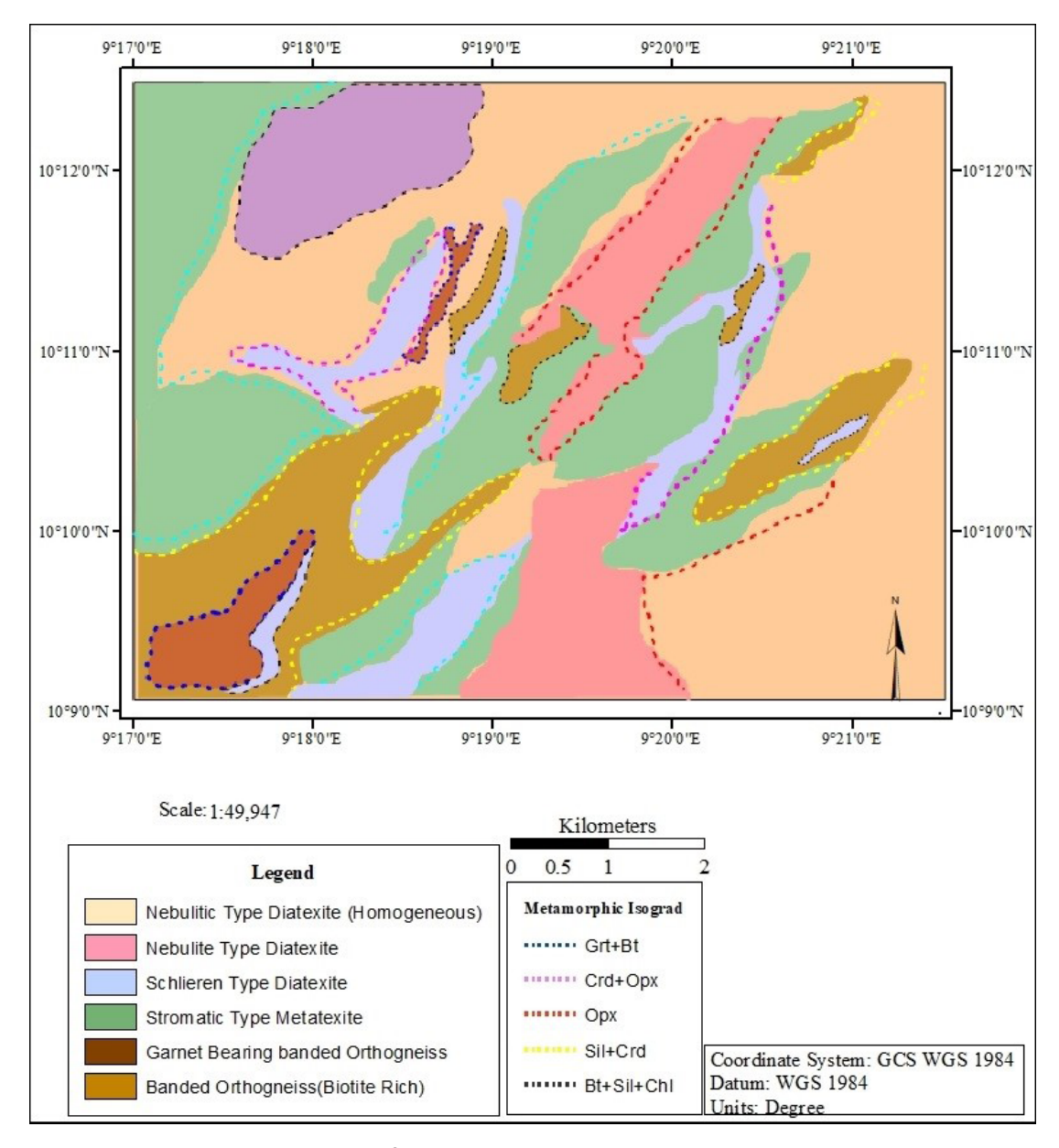


Figure 3. Litho-morphological map of the study area.

Global Mapper Software V16.2 was also used. The image was then exported into Arc-GIS to extract the lineaments. The lineaments generated were further processed and analyzed using Rockware software to produce the rose diagram.

3. Result and Discussion

3.1. Morpho-lithology and texture

The rocks are predominantly migmatite morphologies, which are characterized by consolidated rock matrix forms of secondary aquifers.

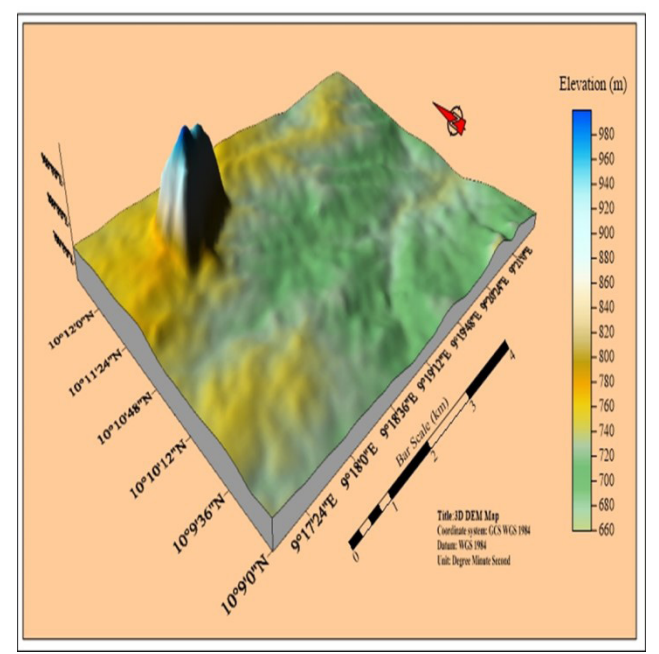
3.1.1. Metatexite

Finely grained in texture, banded, foliated, and very resistant to weathering having biotite and plagioclase

with minor quartz and garnet as the most abundant minerals (Figs. 3 and 5). The presence of foliation in this rock morphology makes it to be the most potential lithology for having pathway geometry that serves as a feeder to the fracture that cut across the rock lithology, hence making it the best conduit in groundwater exploration.

3.1.2. Diatexite

These morphologies are medium-grained in texture. It is believed to have been partially migmatized resulting in distinct felsic and mafic bands (leucosome and melanosome) (Fig. 6a) of a few millimeters to tens of centimeters hence the name diatexite having Quartz, K-feldspar, ±Biotite, and Orthopyroxene as the dominant minerals (Figs. 3 and 6). The common structure



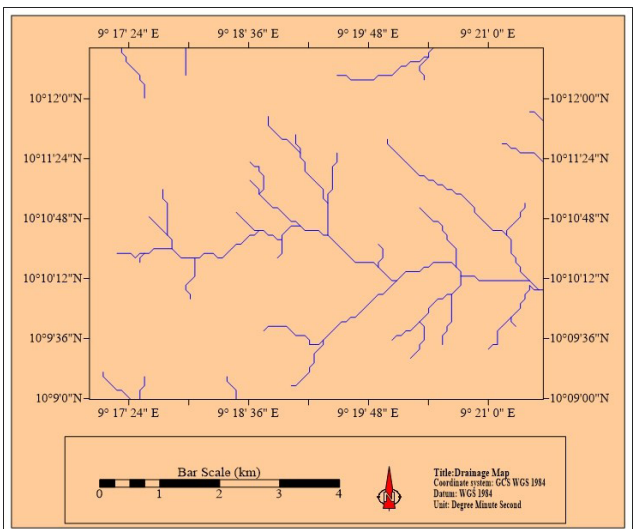


Figure 4. (a) 3D DEM of the study area. (b) Drainage pattern of the study area.

observed in this rock is ptygmatic folding. They occur as massive but show evidence of magmatic foliation which made it a poor conduit for water migration but lesser resistance to weathering. A good conduit of this type is due to fracturing if it occurs in the rock.

3.2. Field observation in relation to analysis of foliation and fracture for groundwater exploration

Surface mapping of structural elements (foliation and fracture) was conducted to establish the different structural and morphological units that will serve as a good water-bearing morphological system. The metatexite has a structural attitude of foliation gently dipping and has a high abundance of jointing which will provide a continuous source of recharge (conduit) in the depression part of the study area (Fig. 7). Diatexite which is found in the peak section (Fig. 7) occurs more massive and structures are almost obliterated that will serve as a pathway for water movement along foliation but will provide water from the jointing system and foliation parallel parting system which are found in proximity to the metatexite. It is studied that water derived from a steeply dipping foliation system provides a yield ranging from 1 to 5 gal/minute.

3.3. Foliation analysis

From the analysis of deformation in the study area, foliation (n=67) (Table 1), mostly collected closer to stream and river, was collected and served as the major structural continuous feature of the migmatite morphology. The foliation within the metatexite shows a structural dipping attitude of around $20^{\circ}-80^{\circ}$ (Fig. 8) and it slows the high abundance of jointing which provides a continuous source of recharge (conduit) along these structural elements. But in diatexite, most of the foliations are obliterated and are compositionally massive but it can provide water from the joint within it and foliation parting which dip steeply around $40^{\circ}-85^{\circ}$ (Figs. 9 and 10).

3.4. Fracture

Analysis of fracture (n = 87) shows that it serves as the major structural continuous conduit that cut across the migmatite morphology in the study area which is represented in Figure 11 another rose plot. The fracture trend NE and sometimes NW cross-cutting the metatexite and diatexite (Table 2).

The major fractures that were observed based on the relationship with foliation within the migmatite morphology are of two types:

3.4.1. Low-yield fracture

These fractures are striking mostly in NNW-SSW trends (Figs. 11 and 13) and are mostly found in the diatexite where the degree of partial melting is high and the proportion of unfoliated layer is less.

3.4.2. High-yield fracture

These fractures are most striking in NNE-SSW and NW-SE direction (Figs. 11 and 13) which is found in metatexite morphology preferably banded orthogneiss.

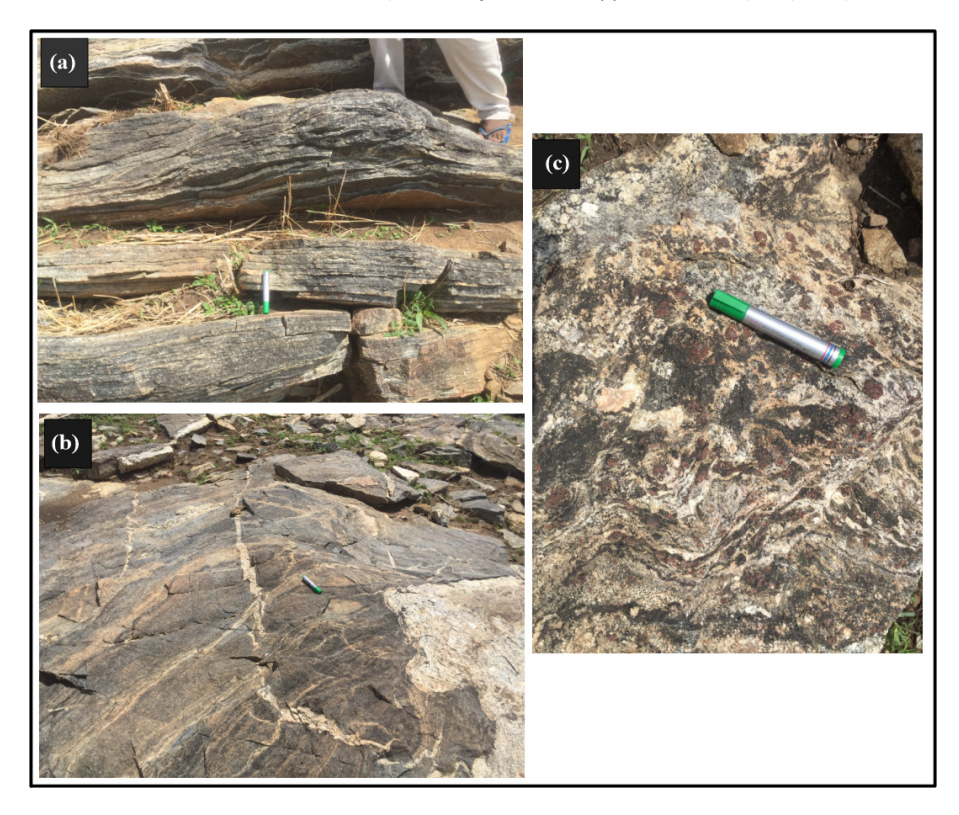


Figure 5. Field photograph showing metatexite. (a) Banded orthogneiss metatexite showing foliation; (b) patch metatexite in field in contact with injected leucosome; and (c) metatexite showing garnet porphyroblast.

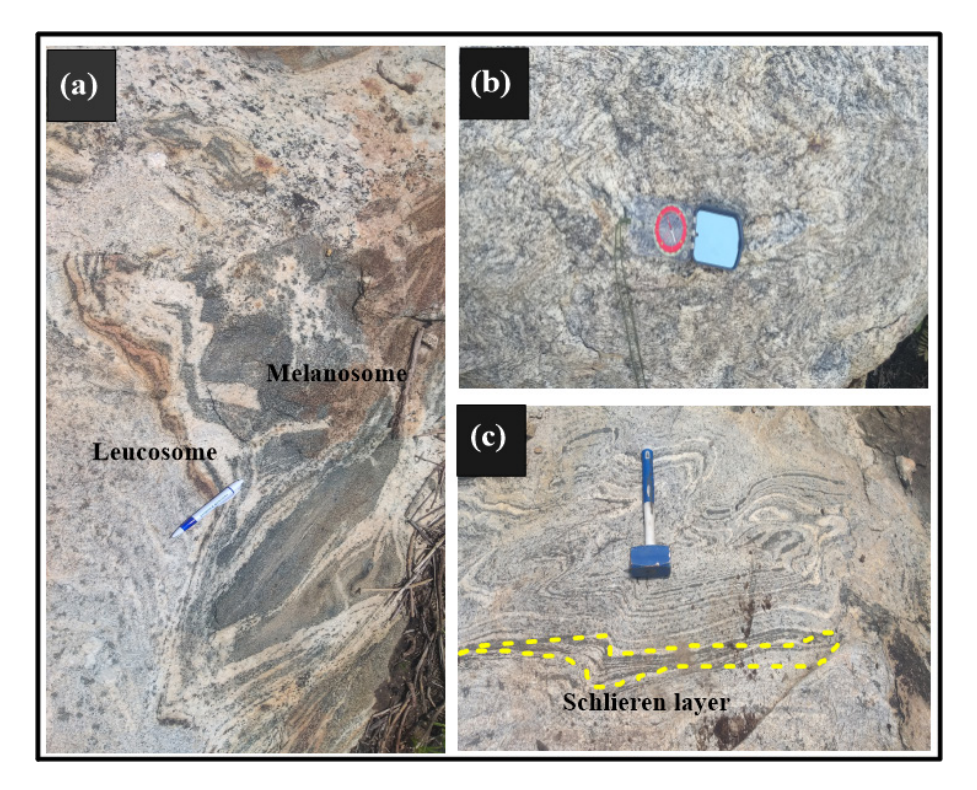


Figure 6. Field photographs showing several aspects of schlieren diatexites. (a) Neosome showing dark the melanosome and leucosome; (b) mesocratic diatexite with crenulation cleavages; and (c) diatexite with abundant schlieric layer.

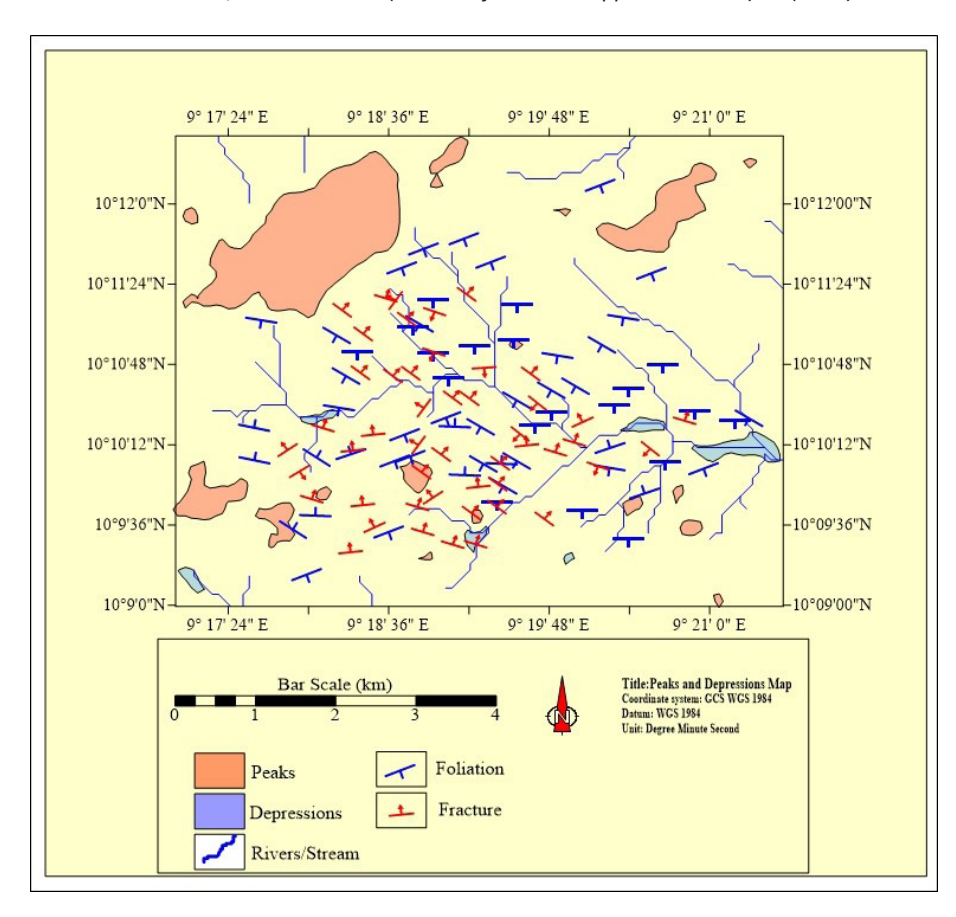


Figure 7. Peak and depression map integrated with structural trend of foliation and fracture of the study area showing areas of high elevation and low with respect to different migmatite morphologies.

Table 1. Foliation type and attitude reading of different migmatite morphological type.

	, · ·	9		0 /.			
S/N	Locality	Structure type	Dip	Dip Azimuth	Strike	Morphology	
1	Rimin Zayam	Foliation plane	44	245	155	Banded orthogneiss	
2	Rimin Zayam	Foliation plane	56	253	163	Banded orthogneiss	
3	Rimin Zayam	Foliation plane	51	246	156	Banded orthogneiss	
4	Rimin Zayam	Foliation plane	40	214	124	Banded orthogneiss	
5	Rimin Zayam	Foliation plane	19	332	242	Banded orthogneiss	
6	Rimin Zayam	Foliation plane	43	224	134	Banded orthogneiss	
7	Gada Biyu	Magmatic foliation	50	223	133	Diatexite	
8	Gada Biyu	Magmatic foliation	49	256	166	Diatexite	
9	Gada Biyu	Magmatic foliation	32	243	153	Diatexite	
10	Gada Biyu	Magmatic foliation	34	259	169	Diatexite	
11	Gada Biyu	Magmatic foliation	13	283	193	Diatexite	
12	Gada Biyu	Magmatic foliation	19	256	166	Diatexite	
13	Gada Biyu	Magmatic foliation	21	216	126	Stomatic metatexite	
14	Gada Biyu	Magmatic foliation	15	233	143	Stomatic metatexite	
15	Gada Biyu	Magmatic foliation	12	249	159	Stomatic metatexite	
16	Gada Biyu	Magmatic foliation	24	241	151	Stomatic metatexite	
17	Gada Biyu	Magmatic foliation	32	256	166	Stomatic metatexite	
18	Gada Biyu	Magmatic foliation	35	234	144	Stomatic metatexite	
19	Gada Biyu	Magmatic foliation	32	225	135	Stomatic metatexite	
20	Gada Biyu	Magmatic foliation	30	219	129	Stomatic metatexite	
						Contin	uad

S/N	Locality	Structure type	Dip	Dip Azimuth	Strike	Morphology
21	Gada Biyu	Magmatic foliation	33	212	122	Stomatic metatexite
22	Gada Biyu	Magmatic foliation	30	236	146	Stomatic metatexite
23	Gada Biyu	Magmatic foliation	33	206	116	Stomatic metatexite
24	Rimin Zayam	Foliation plane	78	232	142	Banded orthogneiss
25	Rimin Zayam	Foliation plane	50	56	326	Banded orthogneiss
26	Rimin Zayam	Foliation plane	61	50	320	Banded orthogneiss
27	Rimin Zayam	Foliation plane	72	85	355	Banded orthogneiss
28	Rimin Zayam	Foliation plane	55	224	134	Banded orthogneiss
29	Rimin Zayam	Foliation plane	59	218	128	Banded orthogneiss
30	Rimin Zayam	Foliation plane	60	48	318	Banded orthogneiss
31	Rimin Zayam	Foliation plane	48	39	309	Banded orthogneiss
32	Rimin Zayam	Foliation plane	32	27	297	Banded orthogneiss
33	Rimin Zayam	Foliation plane	69	71	341	Banded orthogneiss
34	Rimin Zayam	Foliation plane	73	80	350	Banded orthogneiss
35	Gada Biyu	Magmatic foliation	74	85	355	Diatexite
36	Gada Biyu	Magmatic foliation	48	43	313	Diatexite
37	Gada Biyu	Magmatic foliation	39	20	290	Diatexite
38	Gada Biyu	Magmatic foliation	35	52	322	Diatexite
39	Gada Biyu	Magmatic foliation	41	35	305	Diatexite
40	Gada Biyu	Magmatic foliation	74	240	150	Diatexite
41	Gada Biyu	Magmatic foliation	83	67	337	Diatexite
42	Gada Biyu	Magmatic foliation	86	53	323	Diatexite
43	Gada Biyu	Magmatic foliation	86	48	318	Diatexite
44	Rimin Zayam	Foliation plane	51	225	135	Banded orthogneiss
45	Rimin Zayam	Foliation plane	83	214	124	Banded orthogneiss
46	Rimin Zayam	Foliation plane	53	99	9	Banded orthogneiss
47	Rimin Zayam	Foliation plane	72	65	335	Banded orthogneiss
48	Rimin Zayam	Foliation plane	69	69	339	Banded orthogneiss
49	Rimin Zayam	Foliation plane	24	224	134	Banded orthogneiss
50	Rimin Zayam	Foliation plane	44	64	334	Banded orthogneiss
51	Rimin Zayam	Foliation plane	48	72	342	Banded orthogneiss
52	Rimin Zayam	Foliation plane	54	64	334	Banded orthogneiss
53	Rimin Zayam	Magmatic foliation	36	64	334	Stomatic metatexite
54	Rimin Zayam	Magmatic foliation	21	251	161	Stomatic metatexite
55	Rimin Zayam	Magmatic foliation	16	242	152	Stomatic metatexite
56	Rimin Zayam	Magmatic foliation	18	255	165	Diatexite
57	Rimin Zayam	Magmatic foliation	60	254	164	Diatexite
58	Rimin Zayam	Magmatic foliation	58	239	149	Diatexite
59	Rimin Zayam	Magmatic foliation	50	257	167	Diatexite
60	Rimin Zayam	Magmatic foliation	53	241	151	Diatexite
61	Rimin Zayam	Magmatic foliation	47	247	157	Diatexite
62	Rimin Zayam	Magmatic foliation	50	241	151	Diatexite
63	Rimin Zayam	Magmatic foliation	43	232	142	Diatexite
64	Rimin Zayam	Magmatic foliation	47	226	136	Diatexite
65	Rimin Zayam	Magmatic foliation	41	252	162	Diatexite
66	Rimin Zayam	Magmatic foliation	38	255	165	Diatexite
67	Rimin Zayam	Magmatic foliation	30	235	145	Diatexite

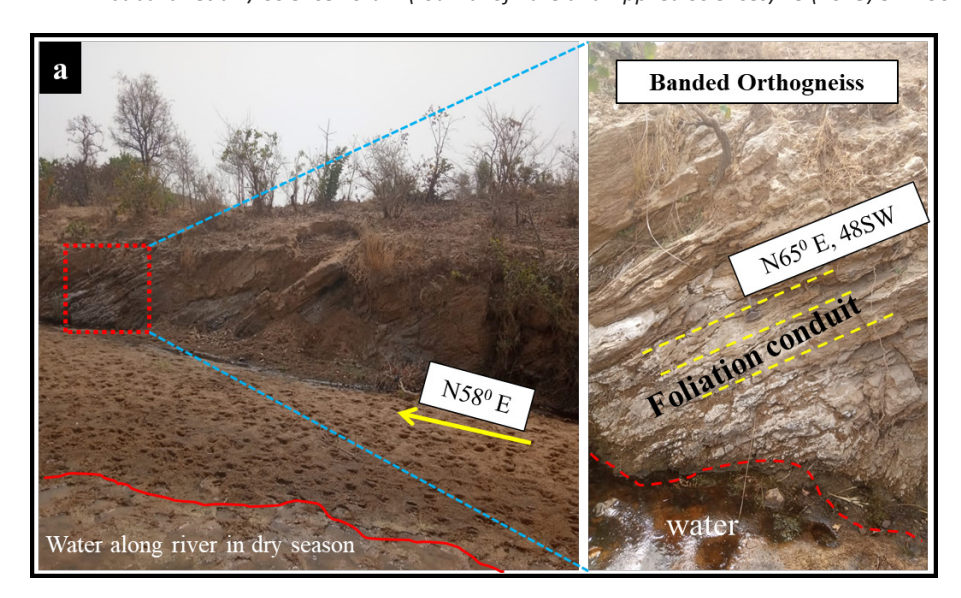


Figure 8. Field picture of weathered banded orthogneiss type metatexite along river channel where the foliation within the metatexite serves as conduit that feeds the river.

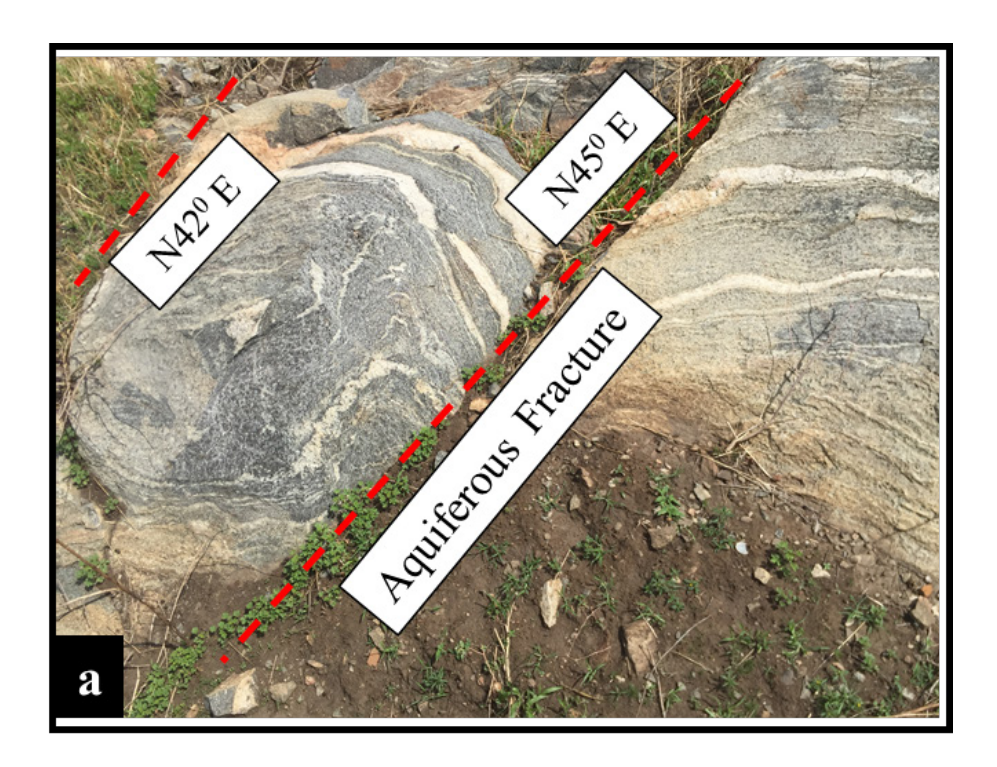
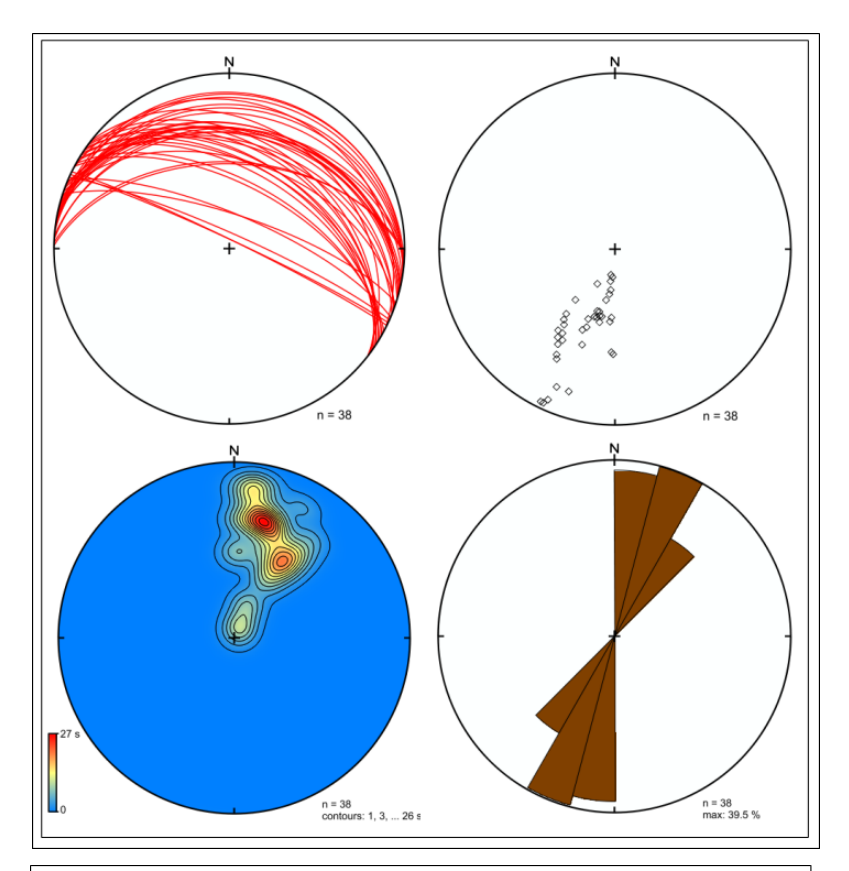


Figure 9. Aquiferous fracture in stromatic migmatite trending N45°E.

In conclusion, the gently dipping foliation in the area $(40^{\circ}-60^{\circ})$ to gather with high-yield fractures will provide a high yield of groundwater and serve as the most water-bearing zone in the area.

3.5. Conceptual model for groundwater zone in the study area

The geometric structural analysis of structures within the different morphology of migmatite in the study area reveals that the geometrics of foliation and fractures in diatexite lack the structural specificity of water yield zone (Fig. 12) from a jointing system only ranging from 1 to 5 gal/mm (USGS) and do not represent an important source for the development of larger water-bearing zones (domestic or hydro-power dam) while the metatexite (Fig. 13) which has the specificity of structural geometry of high-water zone will produce high water yield and the lithology could be tapped for



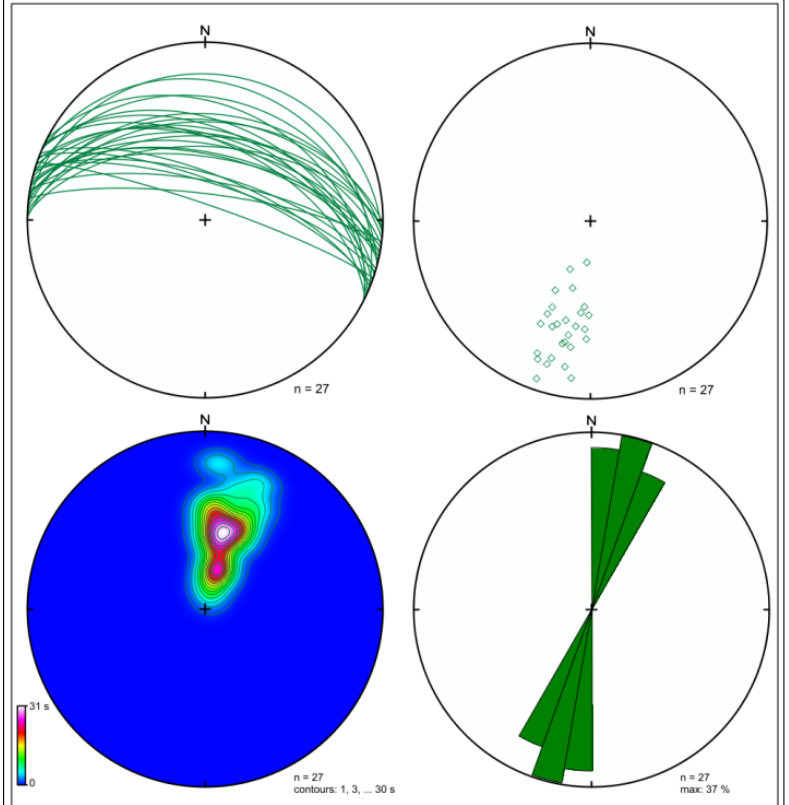


Figure 10. (a) Stereonet plots of possible aquiferous foliation. Red bold cross: beta axis, black point: s-axis, colored contour: calculated girdle of foliation plane, brown histogram: rose plot depicting trend of foliation. (b) Stereonet plots of possible aquiferous fractures. Green bold cross: beta axis, green point: s-axis, colored contour: calculated girdle of fractures, green histogram: rose plot depicting fracture trend.

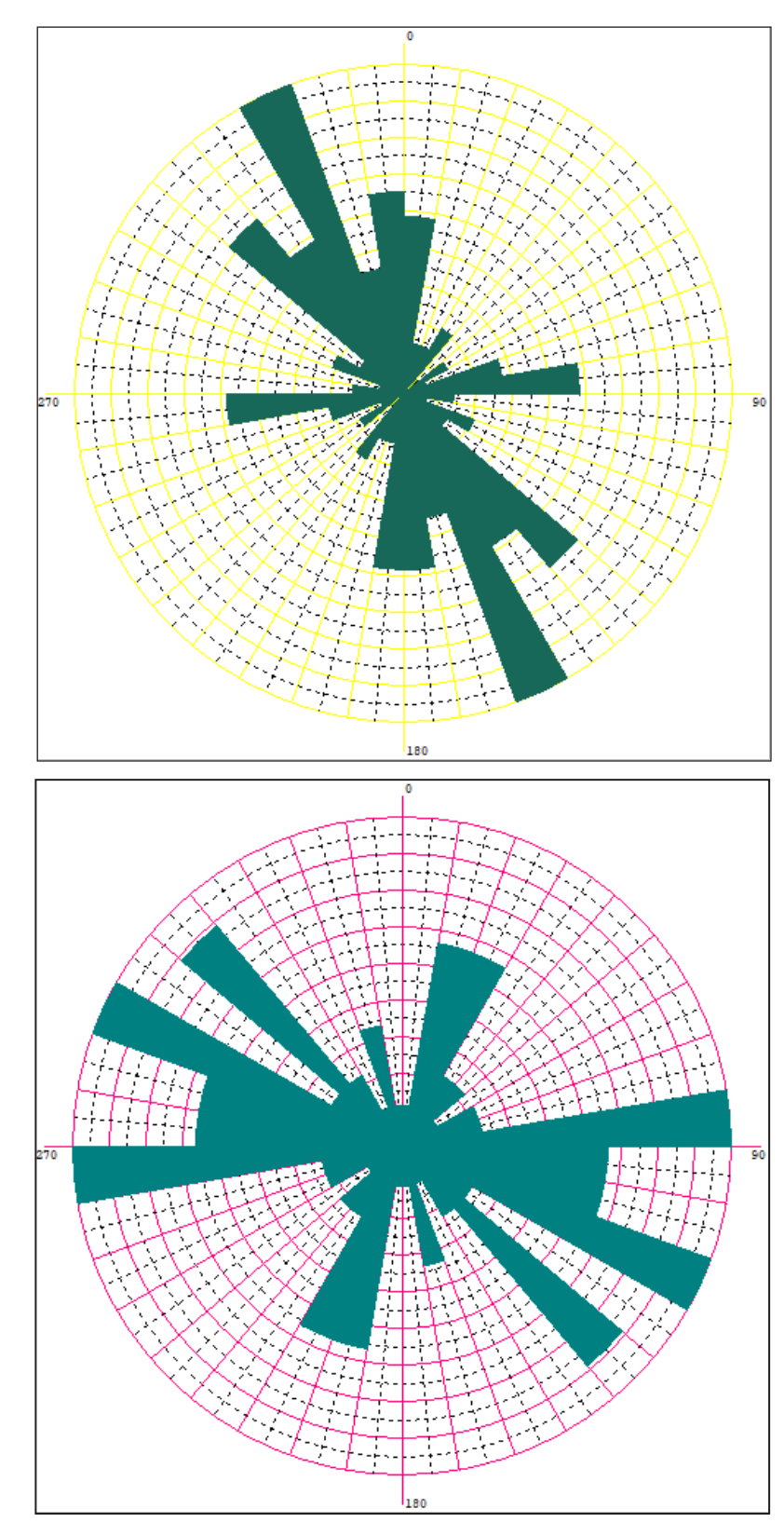


Figure 11. Rose diagram showing the trends of fractures within the study area.

larger water bodies due to the greatest availability of groundwater is gotten from the geometric zone of high

foliation concentration and area of jointing intersect (Fig. 12).

Table 2. Attitude reading of different fractures taken from the migmatite field.

S/N	Location	Strike	Azimuth	Morphology	Fracture yield
1	Rimin Zayam	N40E	220	Stomatic metatexite	Low-yield fracture
2	Rimin Zayam	N346W	166	Stomatic metatexite	High-yield fracture
3	Rimin Zayam	N340W	160	Stomatic metatexite	High-yield fracture
4	Rimin Zayam	N358W	78	Stomatic metatexite	Low-yield fracture
5	Rimin Zayam	N012E	192	Stomatic metatexite	High-yield fracture
6	Rimin Zayam	N034E	214	Stomatic metatexite	High-yield fracture
7	Rimin Zayam	N334W	154	Stomatic metatexite	High-yield fracture
8	Rimin Zayam	N346W	166	Stomatic metatexite	High-yield fracture
9	Rimin Zayam	N340W	160	Stomatic metatexite	High-yield fracture
10	Rimin Zayam	S152E	332	Stomatic metatexite	High-yield fracture
11	Rimin Zayam	N320W	140	Stomatic metatexite	High-yield fracture
12	Rimin Zayam	N338W	158	Banded orthogneiss	High-yield fracture
13	Rimin Zayam	N358W	178	Banded orthogneiss	High-yield fracture
14	Rimin Zayam	S160E	340	Banded orthogneiss	High-yield fracture
15	Rimin Zayam	N300W	120	Banded orthogneiss	High-yield fracture
16	Rimin Zayam	270W	90	Banded orthogneiss	Low-yield fracture
17	Rimin Zayam	N276W	96	Banded orthogneiss	Low-yield fracture
18	Rimin Zayam	90E	270	Banded orthogneiss	High-yield fracture
19	Rimin Zayam	N300W	120	Banded orthogneiss	High-yield fracture
20	Rimin Zayam	S260W	80	Banded orthogneiss	Low-yield fracture
21	Rimin Zayam	N300W	120	Banded orthogneiss	High-yield fracture
22	Rimin Zayam	N340W	160	Banded orthogneiss	High-yield fracture
23	Rimin Zayam	S146E	326	Banded orthogneiss	High-yield fracture
24	Rimin Zayam	N340W	160	Banded orthogneiss	High-yield fracture
25	Rimin Zayam	N320W	140	Banded orthogneiss	High-yield fracture
26	Rimin Zayam	N004E	184	Banded orthogneiss	High-yield fracture
27	Rimin Zayam	N334W	154	Banded orthogneiss	High-yield fracture
28	Rimin Zayam	N344W	164	Banded orthogneiss	High-yield fracture
29	Rimin Zayam	N358W	178	Banded orthogneiss	High-yield fracture
30	Rimin Zayam	N350W	170	Banded orthogneiss	High-yield fracture
31	Rimin Zayam	N010E	190	Banded orthogneiss	High-yield fracture
32	Rimin Zayam	N310W	130	Banded orthogneiss	High-yield fracture
33	Rimin Zayam	N052E	232	Banded orthogneiss	High-yield fracture
34	Rimin Zayam	S150E	330	Banded orthogneiss	High-yield fracture
35	Rimin Zayam	180S	0	Banded orthogneiss	Low-yield fracture
36	Gada Biyu	S140E	320	Banded orthogneiss	High-yield fracture
37	Gada Biyu	N360W	180	Banded orthogneiss	High-yield fracture
38	Gada Biyu	N330W	150	Banded orthogneiss	High-yield fracture
39	Gada Biyu	N340W	160	Banded orthogneiss	High-yield fracture
40	Gada Biyu	N320W	140	Banded orthogneiss	High-yield fracture
41	Gada Biyu	S236W	56	Banded orthogneiss	Low-yield fracture
42	Gada Biyu	N320W	140	Banded orthogneiss	High-yield fracture
43	Gada Biyu	S264W	84	Banded orthogneiss	Low-yield fracture
44	, Gada Biyu	S140E	320	Banded orthogneiss	, High-yield fracture

S/N	Location	Strike	Azimuth	Morphology	Fracture yield
45	Gada Biyu	180S	0	Banded orthogneiss	High-yield fracture
46	Gada Biyu	S136E	316	Diatexite	High-yield fracture
47	Gada Biyu	N350W	170	Diatexite	Low-yield fracture
48	Gada Biyu	S150E	330	Diatexite	High-yield fracture
49	Gada Biyu	N318W	138	Diatexite	High-yield fracture
50	Gada Biyu	N310W	130	Diatexite	High-yield fracture
51	Gada Biyu	N290W	110	Diatexite	High-yield fracture
52	Gada Biyu	N010E	190	Diatexite	Low-yield fracture
53	Gada Biyu	S144E	324	Diatexite	High-yield fracture
54	Gada Biyu	270W	90	Diatexite	Low-yield fracture
55	Gada Biyu	270W	90	Diatexite	Low-yield fracture
56	Gada Biyu	S260W	80	Diatexite	Low-yield fracture
57	Gada Biyu	S260W	80	Diatexite	Low-yield fracture
58	Gada Biyu	S262W	82	Diatexite	Low-yield fracture
59	Gada Biyu	N274W	94	Diatexite	Low-yield fracture
60	Gada Biyu	N320W	140	Diatexite	Low-yield fracture
61	Gada Biyu	N360W	180	Diatexite	Low-yield fracture
62	Gada Biyu	N326W	146	Diatexite	Low-yield fracture
63	Gada Biyu	S190W	10	Diatexite	Low-yield fracture
64	Gada Biyu	S152E	332	Diatexite	High-yield fracture
65	Gada Biyu	N330W	150	Diatexite	Low-yield fracture
66	Gada Biyu	180S	0	Diatexite	Low-yield fracture
67	Gada Biyu	S182W	2	Diatexite	Low-yield fracture
68	Gada Biyu	S184W	4	Diatexite	Low-yield fracture
69	Gada Biyu	S160E	340	Diatexite	High-yield fracture
70	Gada Biyu	S186W	6	Diatexite	Low-yield fracture
71	Gada Biyu	S194W	12	Diatexite	Low-yield fracture
72	Gada Biyu	270W	90	Diatexite	Low-yield fracture
73	Gada Biyu	S250W	70	Diatexite	Low-yield fracture
74	Gada Biyu	N030E	210	Diatexite	Low-yield fracture
75	Gada Biyu	N022E	202	Diatexite	Low-yield fracture
76	Gada Biyu	N039E	219	Diatexite	High-yield fracture
77	Gada Biyu	N340W	160	Diatexite	Low-yield fracture
78	Gada Biyu	S120E	300	Diatexite	High-yield fracture
79	Gada Biyu	N286W	106	Diatexite	Low-yield fracture
80	Gada Biyu	270E	90	Diatexite	Low-yield fracture
81	Gada Biyu	S140E	320	Diatexite	High-yield fracture
82	Gada Biyu	N280W	100	Diatexite	High-yield fracture
83	Gada Biyu	N316W	136	Diatexite	High-yield fracture
84	Gada Biyu	N016E	196	Diatexite	Low-yield fracture
85	, Gada Biyu	N300W	120	Diatexite	, High-yield fracture
86	Gada Biyu	N286W	106	Diatexite	High-yield fracture
87	, Gada Biyu	N320W	140	Diatexite	High-yield fracture
88	, Gada Biyu	N330W	150	Diatexite	High-yield fracture

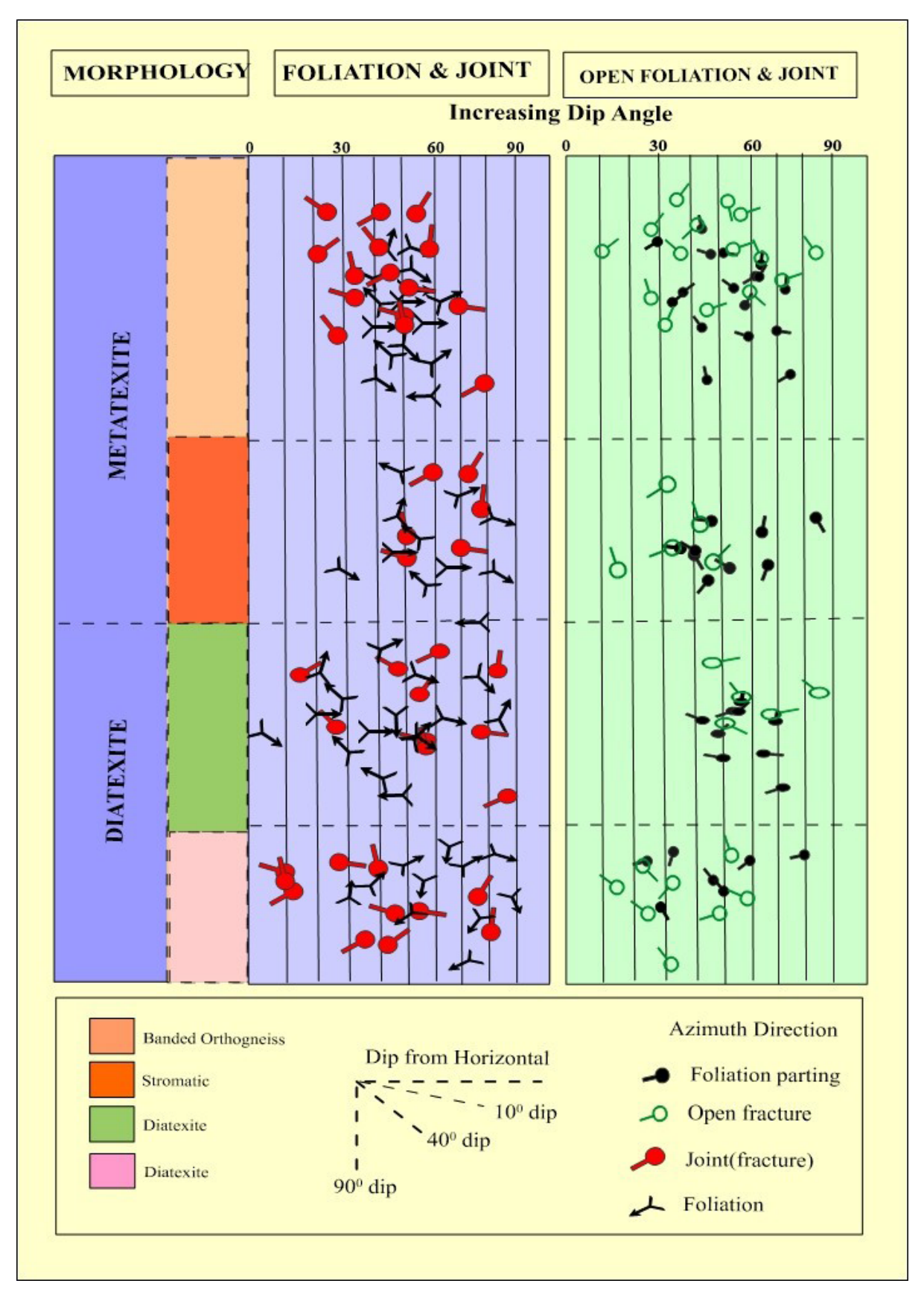


Figure 12. Surface lithological characteristic and structural element plot showing the differences in structural distribution in the different migmatite morphology studied.

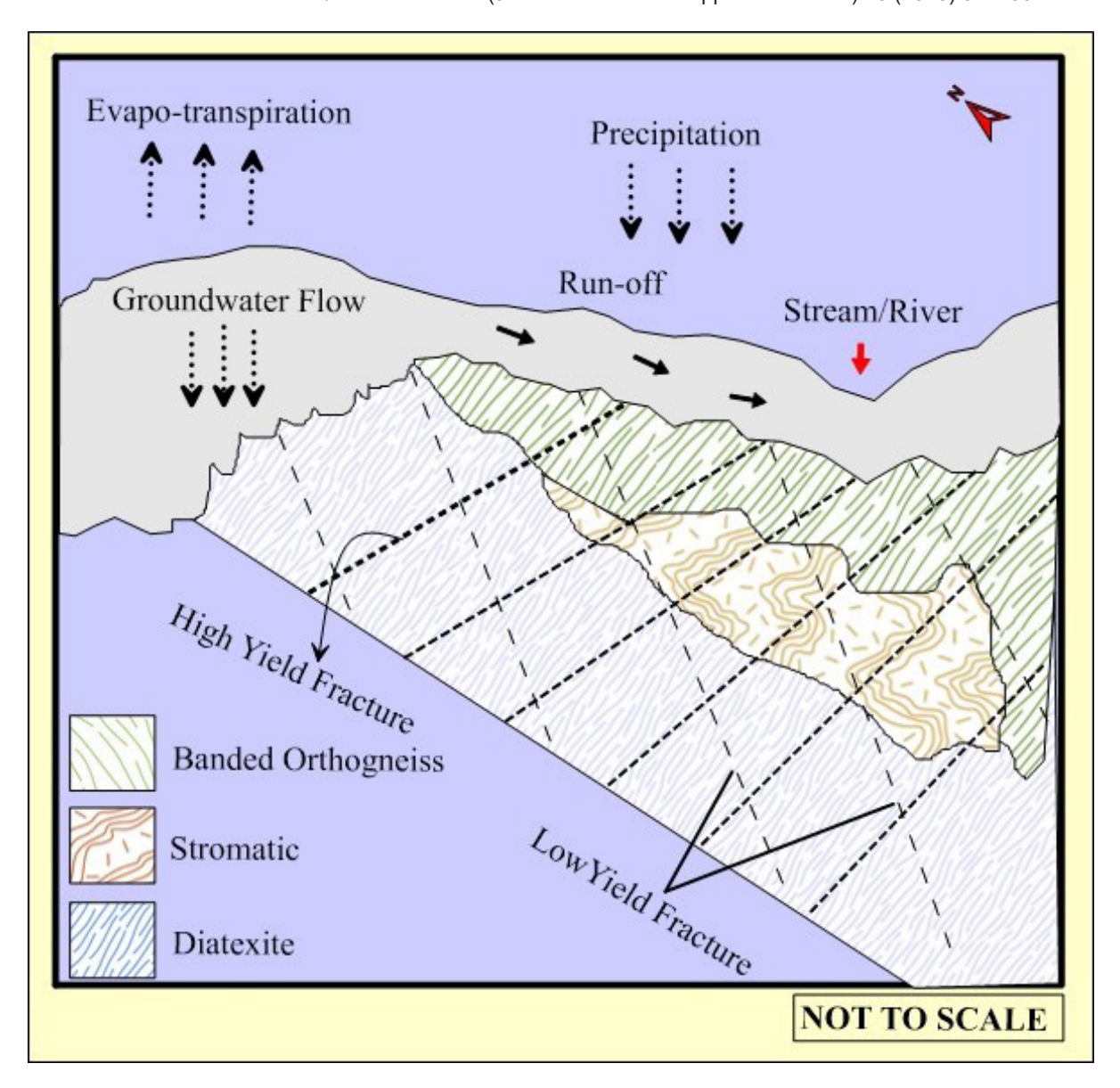


Figure 13. Conceptual groundwater model; showing the different migmatite subdivisions as well as their structural specificity in terms of progressive yield with respect to fracture and lithological variation that are exposed to weathering at outcrop scale.

4. Conclusion

The result obtained from hydrostructural readings of foliation and fracture systems in migmatite show significant and interesting variation regarding foliation/fracture strike conduit specificity in groundwater availability in the study area. This approach should be used as first hand-measured in outcrop to predict the influence of foliation/fracture structural element in modeling groundwater availability in migmatite morphology preferably metatexite due to its high presence of foliation that serves as the most fundamental element controlling groundwater movement in migmatitic rocks than diatexite morphology. Therefore,

migmatite morphology should serve as the heart of generating a hydrostructural map, making correlations, and establishing the hydrogeological history of any area in order to make a possible prediction about groundwater potential for domestic or industrial use. Areas of high-yield fracture serve as good conduits for water migration while low-yield fracture provides a low migration and recharge of water to the neighboring reservoir. Understanding the hydrogeological nature of migmatite morphologies as aquifers, surface heterogeneity, and structural mapping is crucial in utilizing the potential of groundwater in any migmatitic terrane. This method used in this article may

have a great application to other areas of groundwater availability in structurally controlled rock aquifers of interest. In conclusion, there is a lack of understanding of the underlying structural patterns that control groundwater occurrence and the elements determining permeability within the terrain, resulting in ineffective groundwater exploration planning.

Acknowledgments

We thank anonymous reviewers for their constructive comments that helped to improve the manuscript. We are also thankful for the careful editorial guidance and insightful comments and suggestions.

Conflicts of interest

The authors declare that the research was conducted in the absence of any commercial or financial relationships that could be construed as a potential conflict of interest.

Funding

This research received no external funding.

Authors contribution

Faisal Abdullahi performed research, analyzed, and interpreted data, generated the figures, prepared the text, and wrote the manuscript. Tahir Garba also performed research and data analysis. Ahmed Isah Haruna contributed to the interpretation of the results and reviewed the manuscript. Maimunatu Halilu provided materials, contributed to the interpretation of results, and reviewed the manuscript. All authors have read and agreed to the published version of the manuscript.

Reference

- Annor AE, Freeth EJ. Thermotectonic evolution of the basement complex around Okene, Nigeria, with special reference to deformational mechanism. Precamb Res 1985; 28:269–81.
- Brown M. The definition of metatexis, diatexis and migmatite. Proc Geol Assoc 1973; 84:371–82.
- Brown M. Crustal melting and granite magmatism: key issues. Phys Chem Earth A 2001a; 26:201–12.
- Brown M. Orogeny, migmatites and leucogranites: a review. Proc Indian Acad Sci 2001b; 110:313–36.
- Dada SS. Proterozoic evolution of Nigeria. In: Oshin O (Ed.). The basement complex of Nigeria and its mineral resources. Akin Jinad, Ibadan, Nigeria, pp 29–45, 2006.

- Dada SS, Lancelot JR, Briqueu L. Age and origin of the annular Charnockitic complex at Toro, Northern Nigeria: U-Pb and Rb-Sr evidence. J Afr Earth Sci 1989; 9(2):227–34.
- Dada SS, Respaut JP. The fayalite monzonite of Bauchi (bauchite); new evidence of pan-African syntectonic magmatism in northern Nigeria. Rep Acad Sci Ser 1989; 309:887–92.
- Ferre CE, Caby R. Granulite facies metamorphism and charnockite plutonism: examples from the neoproterozoic belt of Northern Nigeria. J Geol 2006; 100:06006.
- Ferre EC, Caby R, Peucat JJ, Capdevila IR, Monie P. Pan-African post-collisional ferro-potassic granite and quartz-monzonite plutons of Eastern Nigeria. Lithos 1998; 45:255–78.
- Ferré EC, Gleizes G, Caby R. Tectonics and post-collisional granite emplacement in an obliquely convergent orogen: the Trans-Saharan belt, Eastern Nigeria. Precambrian Res 2002; 114:199–219.
- Obiora SC. Field descriptions of hard rocks with examples from the Nigerian basement complex. 1st edition, Snap Press, Enugu, Nigeria, p 14, 2005.
- Oyawoye MO. The petrology of the older granites around Bauchi, Nigeria. Theses, Durham University, Durham, UK, 1959.
- Passchier CW, Trouw RAJ. Microtectonics. 2nd edition, Springer-Verlag, Heidelberg, Germany, 2005.
- Rahaman MA. Review of the basement geology of south western Nigeria. In: Kogbe CA (Ed.). Geology of Nigeria, Elizabethan Pub., Lagos, Nigeria, pp 41–58, 1976.
- Rushmer T. Partial melting of two amphibolites: contrasting experimental results under fluid absent conditions. Contr Mineral Petrol 1991; 107(1):41–59.
- Sawyer EW. Melt segregation and magma flow in migmatites: implications for the generation of granite magmas. Earth Environ Sci Trans R Soc Edinb 1996; 87:85–94.
- Sawyer EW. Formation and evolution of granite magmas during crustal reworking: the significance of diatexites. J Petrol 1998; 39:1147–67.
- Sawyer EW. Working with migmatites: nomenclature for the constituent parts. In: Sawyer EW, Brown M (Eds.). Shourt Course, Mineral Association of Canada, Quebec, Canada, pp 1–28, 2008a.
- Sawyer EW. Atlas of migmatites. Mineralogical Association of Canada, Monograph Publishing Program, Quebec, Canada, 321 p, 2008b.
- Sawyer EW, Brown M. (Eds.). Working with migmatites. Mineralogical Association of Canada Short Course, Quebec, Canada, vol. 8, 158 p, 2008.
- Wright JB. Geology and mineral resources of West Africa. George Allen and Unwin, London, UK, p 187, 1985.